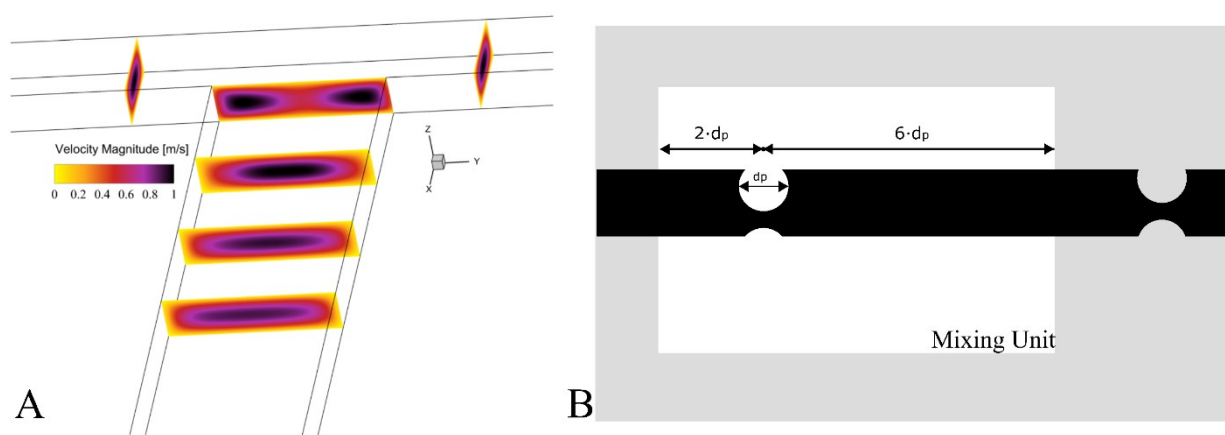# Optimized Design of Obstacle Sequences for Microfluidic Mixing in an Inertial Regime

(Supplementary Information)

Matteo Antognoli, Daniel Stoecklein, Chiara Galletti, Elisabetta Brunazzi and Dino Di Carlo

SI Figure 1 – (A) Before the fluid hit the first pillar in the sequence a length of $400\ \mu m$ was set to ensure a developed parabolic profile of the velocity field after the junction. (B) Spatial configuration of a mixing unit made by one full pillar (top visual).
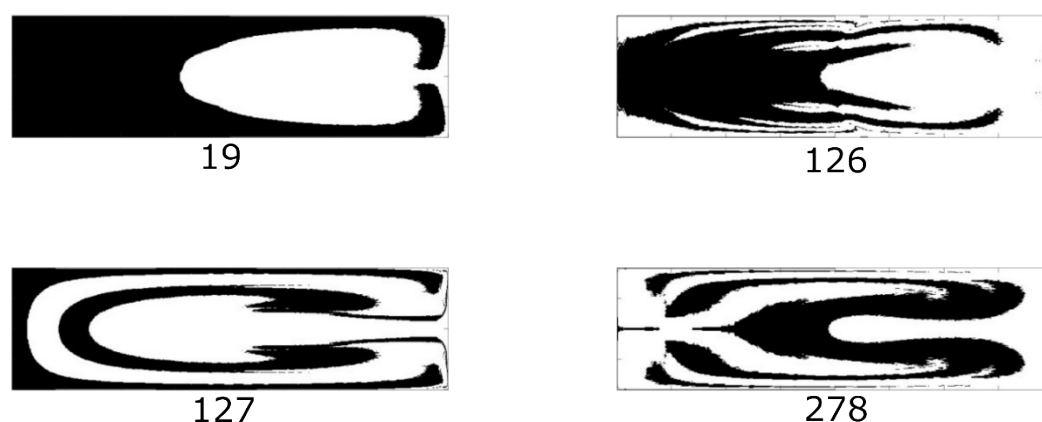

SI Figure 2 – Fluid flow shape predicted by Flowsculpt and values of the Interface Stretching Function.

## Defining computational grids for CFD simulations

As it has been observed in precedent works[1-3], inertial flow regimes in microchannel with pillars have shown a symmetric motion with respect to the middle plan of the channel height. In this work, a symmetry plan was placed at $\frac{H}{2} = 0.025mm$, reducing the size of the domain and the computational time of 3D-CFD simulations. For each optimal sequence, the unstructured grid was firstly built in Gmsh[4] using hexahedral elements and, then, it was exported to be read by ANSYS Fluent v19.2. The outlet section of $25x200\ \mu m^2$ needed to be composed at least of $15x50$ hexahedral elements to accurately describe the velocity field at $Re = 40$.

We tested different grid densities on a small domain (made of one pillar and a T-junction) to accurately estimate the mixing index (MI), which depends on the standard deviation of the passive scalar concentration

field on a specific cross-section. In such domain, a tangent pillar of $150 \mu m$ was defined, and CFD simulations were carried out to evaluate the MI at the outlet using $Pe = 10^5$ changing the total number of elements (see SI Figure 3A). A stable value of MI – error with respect to our finest grid was less than 1% – was found using $20x60$ elements on the outlet section, which corresponded to a domain made of $1.2M$ of hexahedral elements. It is worth mentioning that all created meshes were refined in the regions near to pillars to well compute the higher gradients of velocity and scalar concentration in the channel restrictions (see SI Figure 3B).

In SI Figure 3C velocity streamlines and cross-sectional distributions of passive scalar are represented. We can observe that the velocity strongly increases within the restriction $50x50 \ \mu m^2$, and behind the tangential pillar a stable recirculation is developed. Meanwhile, concentration field is well described over different cross sections showing a U-shaped distribution along the pillar downstream sections.
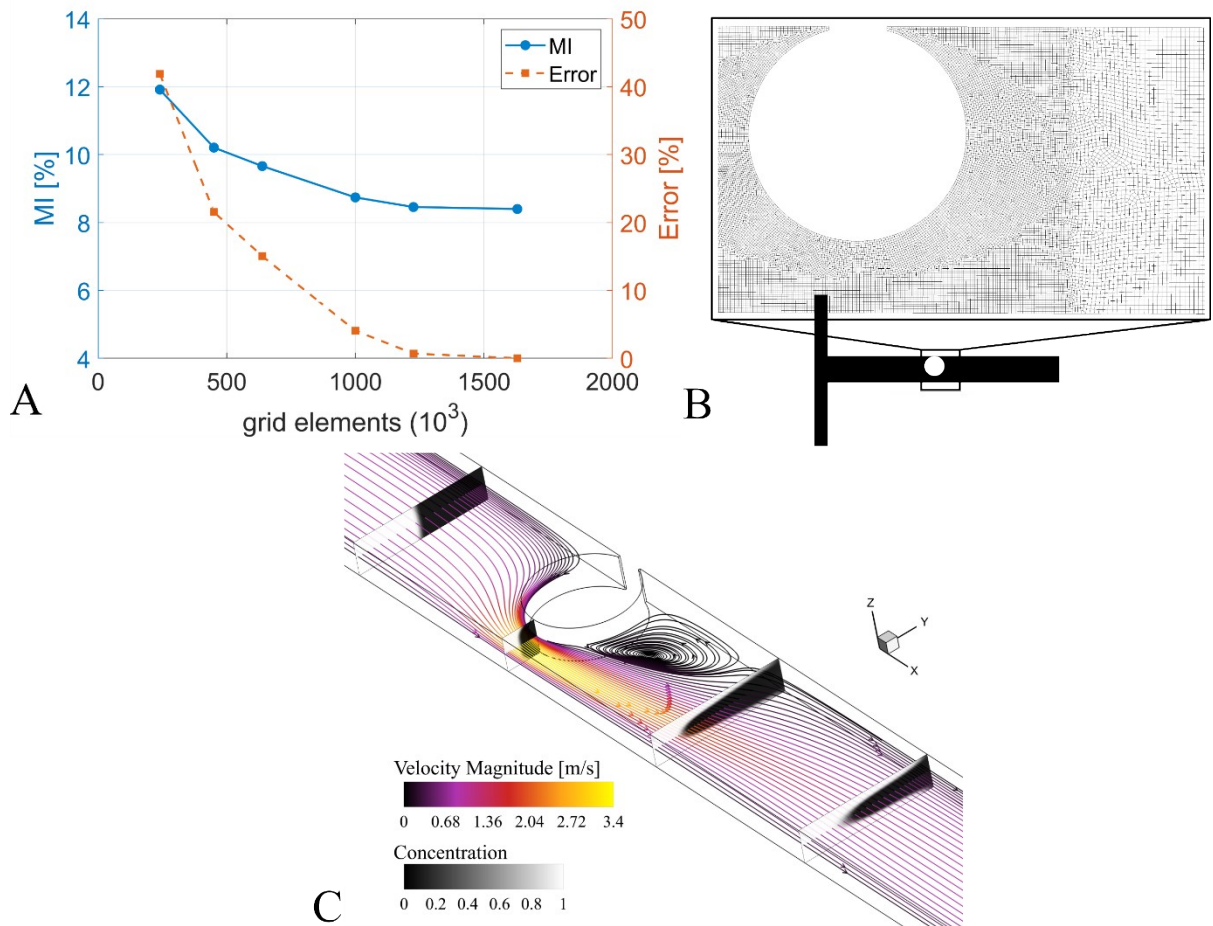
SI Figure 3 (A) – Testing different number of hexahedral elements in a single pillar domain ($D_p = 150 \ \mu m$ and $Y_p = 25 \ \mu m$) and evaluating the mixing index at the exit section at $Re = 40$. (B) Mesh around the tangent pillar is finer that in the other part of the domain. (C) Streamlines with velocity contour and the concentration distribution along cross-sections at $Re = 40$ and $Pe = 10^5$.
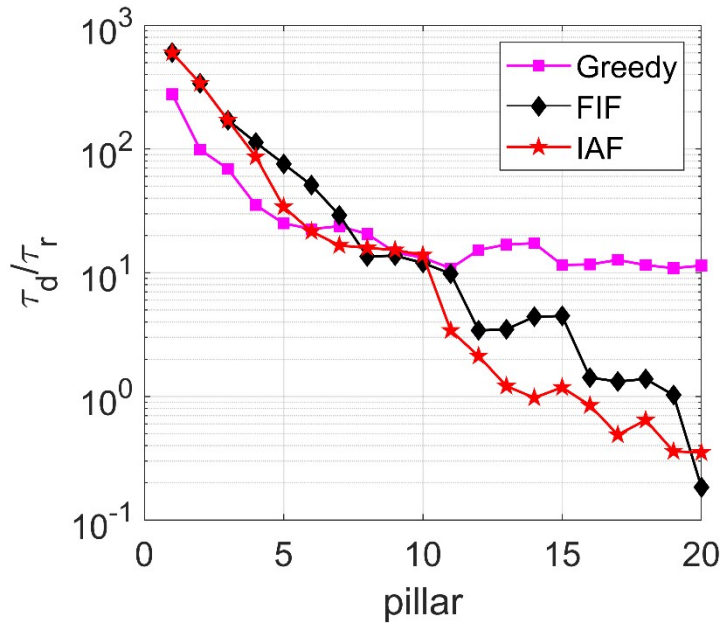
SI Figure 4 – Competition between the mean residence time τ_r and the time to diffuse τ_d through the maximum thickness of dyed fluid striation evaluated by the ISF in FlowSculpt at each cross-section in the post-pillar region.

SI Table 1 – Mixing performances of all optimal sequences using different Péclet numbers (CFD data analysis)

Péclet	MI_{Greedy}	MI_{FIF}	MI_{IAF}
50000	50.1%	86.5%	86.0%
100000	45.0%	81.2%	84.0%
500000	40.1%	74.4%	80.5%

References

1) H. Amini, E. Sollier, M. Masaeli, Y. Xie, B. Ganapathysubramanian, H. A. Stone and D. Di Carlo, Nature Communications,2013

2) D. Stoecklein, C.-Y. Wu, D. Kim, D. Di Carlo and B. Ganapathysubramanian,Physics of Fluids, 2016

3) D. Stoecklein, M. Davies, J. M. De Rutte, C. Y. Wu, D. Di Carlo and B. Ganapathysubramanian, Lab Chip, 2019

4) C. Geuzaine and J.-F. Remacle. International Journal for Numerical Methods in Engineering 79(11), pp. 1309-1331, 2009